



ELSEVIER

Contents lists available at ScienceDirect

Ad Hoc Networks

journal homepage: www.elsevier.com/locate/adhoc

Spectrum Sensing in small-scale networks: Dealing with multiple mobile PUs



Angela Sara Cacciapuoti*, Marcello Caleffi

Department of Electrical Engineering and Information Technology (DIETI), University of Naples Federico II, Italy

ARTICLE INFO

Article history:

Received 25 November 2014

Received in revised form 20 March 2015

Accepted 13 May 2015

Available online 20 May 2015

Keywords:

Mobility

Spectrum Sensing

Cognitive Radio

ABSTRACT

The emerging applications of the small-scale primary-user (PU) paradigm require Cognitive Radio (CR) networks to explicitly support the mobility of a multitude of PUs, concurrently using the same spectrum band. In this paper, the effects of multiple mobile PUs on the spectrum sensing functionality are analyzed to jointly maximize the sensing efficiency and the sensing accuracy. To this aim, as first, a new mathematical model (the aggregate PU model) is proposed to effectively describe the cumulative effects of multiple mobile PUs on the spectrum sensing functionality. Then, stemming from this model, closed-form expressions for the sensing time and the transmission time that jointly maximize the sensing efficiency and the sensing accuracy are derived. Through the derived closed-form expressions, the following fundamental questions are answered: (i) How long can a CR user transmit without interfering with the multiple mobile PUs? (ii) How long must a CR user observe a targeted spectrum band to reliably detect multiple mobile PUs? All the theoretical results are derived by adopting a general mobility model for the multiple mobile PUs. The analytical results are finally validated through simulations.

© 2015 Elsevier B.V. All rights reserved.

1. Introduction

Spectrum Sensing is a key functionality in Cognitive Radio (CR) networks [1,2]. Through spectrum sensing, unlicensed users (CR users) can recognize and dynamically exploit portions of the radio spectrum whenever they are vacated by licensed users, referred to as Primary Users (PUs).

The main objective of spectrum sensing is to provide spectrum opportunities to CR users without interfering with the primary network. Consequently, the sensing accuracy and the sensing efficiency are considered key factors for the overall performance of a CR network [1,3].

Since it is widely recognized that the sensing time parameters, i.e., the *sensing time* and the *transmission time*, influence both the sensing accuracy and the sensing efficiency [4,3,5,1,6], a proper selection of the sensing time parameters is necessary.

In this paper, we derive closed-form expressions for the values of the sensing time and the transmission time that jointly maximize the sensing efficiency and the sensing accuracy in presence of multiple mobile PUs using the same spectrum band.

More in detail, as first, we propose a new mathematical model to effectively describe the cumulative effects of multiple mobile PUs on the spectrum sensing functionality. In fact, due to the distinctive features of the CR paradigm, it is not possible to utilize results available in the classical communication network paradigms to model the interaction among multiple mobile PUs and an arbitrary CR user (Section 4.1). Specifically, we develop the concept

* Corresponding author.

E-mail addresses: angelasara.cacciapuoti@unina.it (A.S. Cacciapuoti), marcello.caleffi@unina.it (M. Caleffi).

of *aggregate PU* (Definition 6 in Section 4.1) to represent in a compact form the overall mobility pattern generated by the multiple mobile PUs.

Then, stemming from these results, we analytically derive the criteria for tuning the sensing time and the transmission time to jointly maximize the sensing efficiency and the sensing accuracy. More in detail, we derive closed-form expressions for both the sensing time parameters that allow us to answer the following questions: (i) How long can a CR user transmit without interfering with the multiple mobile PUs? (ii) How long must a CR user observe a targeted spectrum band to reliably detect multiple mobile PUs? Such closed-form expressions reveal a non-linear dependence of the sensing and transmission times from the mobility patterns and the traffic activities of the multiple mobile PUs.

All the theoretical results are derived by adopting a general PU mobility model, in order to assure generality to the analysis.

In a nutshell, the main contributions made in this paper are: (i) the development of the aggregate PU model for describing the cumulative effects of multiple PUs on the spectrum sensing functionality; (ii) the derivation of closed-form expressions for the overall mobility pattern generated by the PUs roaming according to a general mobility model; (iii) the derivation of closed-form expressions for both the sensing time parameters that jointly maximize the sensing efficiency and the sensing accuracy in presence of multiple mobile PUs.

The rest of the paper is organized as follows. In Section 2, we discuss the related work. In Section 3, we describe the system model along with some preliminaries. In Section 4, we develop the aggregate PU model and we derive closed-form expressions for the overall mobility pattern generated by the multiple PUs. These results are used in Section 5 to set the sensing time parameters according to the dynamics and traffic activities of multiple mobile PUs. We validate the analytical results by simulation in Section 6. In Section 7, we conclude the paper, and, finally, some proofs are provided in the appendices.

2. Related Work

So far, the majority of research in spectrum sensing focuses on improving the sensing accuracy and the sensing efficiency by setting the sensing time parameters under the assumption of static CR and PU networks [4,3,5,7,8].

Contrary to such a common assumption, the emerging of a plethora of key applications for the small-scale PU paradigm,¹ e.g., military applications, requires to explicitly account for the mobility of the PUs. Specifically, since mobility changes dynamically the mutual distances among the PUs and the CR users, the mobility varies in time the CR user capability to sense the PU transmissions [6,10,11]. Hence, the spectrum sensing functionality must tune its sensing time parameters according to the mobile PU dynamics to

assure both sensing accuracy and sensing efficiency, as recently proved in [6].

Specifically, [6] the problem of setting of the sensing time parameters in mobile environments is addressed. Nevertheless, the derived results cannot be applied when the small-scale PU paradigm is considered. In fact, the analysis in [6] is carried out by assuming a single PU using the targeted spectrum band. Such a hypothesis is not realistic in small-scale PU scenarios due to the joint effects of short PU transmission range and PU mobility.

3. Assumptions and Preliminaries

In this section, we collect some definitions that will be used through the paper, and we describe the adopted network model.

Definition 1. With reference to a targeted spectrum band, two are the spectrum occupancy models:

- *Single PU for Band (SPB) spectrum occupancy model:* there is only one PU roaming within the network region using the targeted band;
- *Multiple PU for Band (MPB) spectrum occupancy model:* there are multiple PUs roaming within the network region sharing the targeted band.

3.1. Network Model

In this paper we adopt the MPB spectrum occupancy model. Specifically, $\Pi \triangleq \{PU_i\}_{i=1}^N$ denotes the set of N PUs moving according to a general mobility model, independently of each other, in a network region \mathbf{A} and using the same spectrum band. The PU mobility patterns are identically distributed.² R and $f_{\mathbf{x}_{PU}}(\mathbf{x}_{PU})$ denote the protection radius³ and the probability density function (pdf) of the steady-state spatial distribution of an arbitrary PU, respectively. The traffic of the i -th PU is modeled as a two state birth-death process [3,11,6], with death rate α_i and birth rate β_i . In the “on” state PU_i is active with probability $P_{on,i} = \beta_i / (\alpha_i + \beta_i)$, whereas in the “off” state it is inactive with probability $P_{off,i} = \alpha_i / (\alpha_i + \beta_i)$.

The CR users are assumed static and uniformly distributed in the network region \mathbf{A} . $f_{\mathbf{x}_{CR}}(\mathbf{x}_{CR})$ denotes the pdf of the CR user spatial distribution.

3.2. Preliminaries

Let us consider an arbitrary PU, say PU_i , moving in the network region \mathbf{A} according to its steady-state spatial distribution.

² The identical distribution assumption is verified by a large number of very popular mobility models, as for example the random walk and its derivatives, the random waypoint and the random direction mobility model [12]. Moreover, it is not restrictive, since it can be removed and the following analysis continues to hold by easily extending the derived results.

³ To avoid harmful interference against the PUs, the CR users should detect active PUs within a range, referred to as *protection range*, determined by the PU transmission range and by the CR interference range [4,13,6].

¹ Small-scale PU networks include ad hoc networks, wireless personal area networks, and wireless microphones [1,9].

Definition 2. An arbitrary CR user is inside the protection range R of PU_i if PU_i is placed within a disk $\mathbf{C}(\mathbf{x}_{CR})$ of radius R around the CR user location \mathbf{x}_{CR} , i.e., if the Euclidean distance between the CR user and PU_i is not greater than R . In the following, we refer to $\mathbf{C}(\mathbf{x}_{CR})$ as *CR interference region*.

We observe that the value of R mainly depends on the PU transmission power, the CR sensitivity, and the adopted channel model [14]. Hence, the widely-adopted geometric model [14–17] used in Definition 2 allows us to account for the aforementioned system/environmental parameters.

Definition 3. Here we provide the definitions of the main parameters characterizing the patterns of an arbitrary mobility model.

- The out time Θ_i denotes the random time interval PU_i spends out of the interference region of an arbitrary CR user.
- The sojourn time S_i denotes the random time interval PU_i spends inside the interference region of an arbitrary CR user.
- The inter-arrival time $\mathcal{T}_i = S_i + \Theta_i$ denotes the random time interval between two consecutive arrivals of PU_i in the interference region of an arbitrary CR user.
- The arrival rate λ_i is the random arrival rate of PU_i in the interference region of an arbitrary CR user, and it is equal to the inverse of the inter-arrival time, i.e., $\lambda_i \triangleq 1/\mathcal{T}_i$.

In [6] the average value of \mathcal{T}_i , λ_i , S_i and Θ_i are derived by assuming the SPB model, i.e., by assuming that PU_i is the only PU roaming in the network region using the targeted spectrum band. Due to the identical distribution of the PU mobility patterns, it results: $\overline{\mathcal{T}}_{SPB} \triangleq E[\mathcal{T}_i]$, $\overline{\lambda}_{SPB} \triangleq E[\lambda_i]$, $\overline{S}_{SPB} \triangleq E[S_i]$, and $\overline{\Theta}_{SPB} \triangleq E[\Theta_i]$ for any PU_i in Π .

Definition 4. The maximum interference probability $P_{int,i}$ denotes the maximum value of the interference probability that PU_i can tolerate on its transmissions.

Definition 5. The sensing efficiency η is the ratio between the time devoted to the CR transmissions T_{Tx} (transmission time) and the sensing period T_{sp} :

$$\eta \triangleq \frac{T_{Tx}}{T_{sp}} \triangleq \frac{T_{Tx}}{T_s + T_{Tx}} \quad (1)$$

where T_{sp} is defined as the sum of the time devoted to the sensing T_s (sensing time) and the time devoted to the CR transmissions.

4. Aggregate Primary-User: An overall perspective

Here, first we present the *Aggregate PU* model in Section 4.1. Then, in Section 4.2, we characterize the aggregate PU mobility pattern. These results will be used in Section 5 for singling out the criteria for a proper tuning of the sensing time parameters in small-scale PU networks.

4.1. Aggregate PU Model

Let us consider the whole set $\Pi \triangleq \{PU_i\}_{i=1}^N$ of PUs roaming according to a general mobility model in the network region \mathbf{A} , starting from their steady-state spatial distribution.

Definition 6 (Aggregate PU). The aggregate PU is a model for describing the overall mobile pattern generated by the N PUs roaming in the network region \mathbf{A} . Specifically, the aggregate PU is considered inside an arbitrary CR interference region if at least one of the N PUs roaming in the network region \mathbf{A} is inside the CR interference region.

Definition 7. Here we provide the definitions of the main parameters characterizing the mobility patterns of the aggregate PU.

- The aggregate out time Θ_{MPB} denotes the random time-interval the aggregate PU spends out of the CR interference region, i.e., according to Definition 6, the random time interval in which no PU belonging to Π is inside the interference region of an arbitrary CR user.
- The aggregate sojourn time S_{MPB} denotes the random time interval the aggregate PU spends inside the CR interference region, i.e., according to Definition 6, the random time interval in which at least one $PU \in \Pi$ is inside the interference region of an arbitrary CR user.
- The aggregate inter-arrival time $\mathcal{T}_{MPB} = S_{MPB} + \Theta_{MPB}$ denotes the random time interval between two consecutive arrivals of the aggregate PU within the interference region of an arbitrary CR user.
- The aggregate arrival rate λ_{MPB} denotes the random arrival rate of the aggregate PU within the interference region of an arbitrary CR user, and it is equal to the inverse of the aggregate inter-arrival time, i.e., $\lambda_{MPB} \triangleq 1/\mathcal{T}_{MPB}$.

Remark 1. According to the well-known results of the queuing theory, the overall inter-arrival time of N mobile nodes within the range of another arbitrary node can be easily calculated as the inverse of the sum of the single arrival rates⁴ [18]. This result cannot be used to derive the aggregate inter-arrival time, for the distinctive features of the CR paradigm. As an example, let us consider the case depicted in Fig. 1, where Π is constituted by two PUs. Fig. 1 shows PU_2 arriving within the CR interference region during the PU_1 sojourn time. Hence, the PU_2 arrival does not contribute to decrease the aggregate inter-arrival time but it causes the increasing of the aggregate sojourn time, as shown by the green rectangles.

4.2. Aggregate PU mobility characterization

Stemming from the aggregate PU model presented in Section 4.1, here we characterize the overall mobility

⁴ When the arrivals are independent, the overall inter-arrival time is simply equal to $1/(\lambda_1 + \dots + \lambda_N)$.

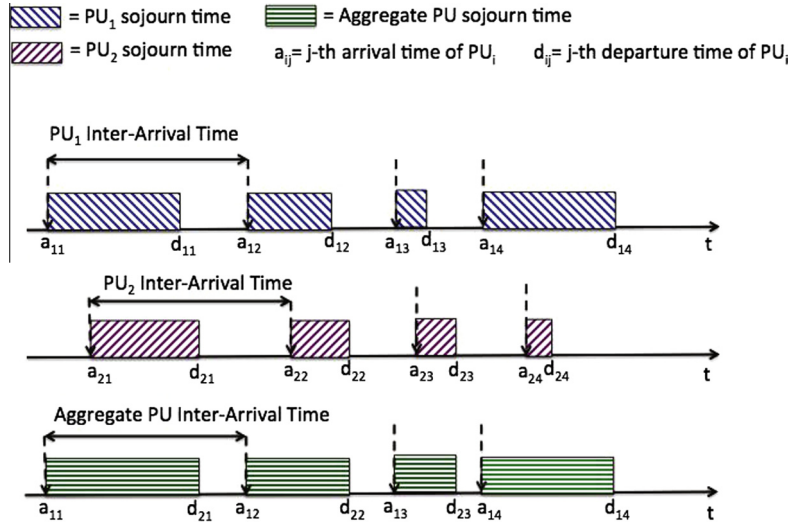


Fig. 1. Aggregate PU mobility pattern: whenever PU_2 arrives within the CR interference region during the PU_1 sojourn times, the PU_2 arrivals do not contribute to decrease the aggregate inter-arrival time.

pattern generated by the PUs in Π , by deriving closed-form expressions for the average aggregate inter-arrival rate (Theorem 1), the average aggregate sojourn time (Proposition 1) and the average aggregate out time (Proposition 2).

In order to prove Theorem 1 and Propositions 1 and 2, Lemma 1 (based on Eq. (6) in [6]) and Lemma 2 (based on Eq. (24) in [11]) are required, along with Definition 8.

Definition 8. Through the paper, the following events are taken into account:

- Event \mathcal{I}_{SPB} : an arbitrary CR user is inside the protection range of an arbitrary PU.
- Event \mathcal{O}_{SPB} : an arbitrary CR user is out of the protection range of an arbitrary PU.
- Event \mathcal{I}_{MPB} : an arbitrary CR user is inside the protection range of at least one PU in Π , i.e., the CR user is inside the protection range of the aggregate PU.
- Event \mathcal{O}_{MPB} : an arbitrary CR user is out of the protection range of any PU in Π , i.e., the CR user is out of the protection range of the aggregate PU.

Lemma 1. The average arrival rate $\bar{\lambda}_{SPB}$ of an arbitrary PU in Π in the interference region of a CR user is equal to:

$$\bar{\lambda}_{SPB} = \frac{1 - P(\mathcal{I}_{SPB})}{\bar{D} \int_{\mathbf{A}} \frac{f_{\mathbf{x}_{CR}}(\mathbf{x}_{CR}) d\mathbf{x}_{CR}}{\int_{\mathcal{C}(\mathbf{x}_{CR}, l)} f_{\mathbf{x}_{PU}}(\mathbf{x}_{PU}) d\mathbf{x}_{PU} f_L(l) dl}} \quad (2)$$

where $P(\mathcal{I}_{SPB})$ is the probability of the event \mathcal{I}_{SPB} , $f_L(l)$ is the pdf of the random variable representing the Euclidean distance covered by the PU during a movement period, and \bar{D} is the average value of the random variable D representing the time spent by the PU to complete a movement [6].

Lemma 2. The probability of event \mathcal{I}_{MPB} is equal to:

$$\begin{aligned} P(\mathcal{I}_{MPB}) &= 1 - P(\mathcal{O}_{MPB}) = 1 - \int_{\mathbf{A}} (1 - P(\mathcal{I}_{SPB}|\mathbf{x}_{CR}))^N f_{\mathbf{x}_{CR}}(\mathbf{x}_{CR}) d\mathbf{x}_{CR} \\ &= \sum_{k=1}^N \binom{N}{k} \int_{\mathbf{A}} P(\mathcal{I}_{SPB}|\mathbf{x}_{CR})^k (1 - P(\mathcal{I}_{SPB}|\mathbf{x}_{CR}))^{N-k} f_{\mathbf{x}_{CR}}(\mathbf{x}_{CR}) d\mathbf{x}_{CR} \end{aligned} \quad (3)$$

where $P(\mathcal{I}_{SPB}|\mathbf{x}_{CR}) \triangleq \int_{\mathcal{C}(\mathbf{x}_{CR})} f_{\mathbf{x}_{PU}}(\mathbf{x}_{PU}) d\mathbf{x}_{PU}$, with $\mathcal{C}(\mathbf{x}_{CR})$ defined in Definition 2.

Theorem 1 (Average Aggregate Arrival Rate). The average aggregate arrival rate $\bar{\lambda}_{MPB}$ of the PUs in Π roaming within the network region \mathbf{A} according to a general mobility model is given by:

$$\begin{aligned} \bar{\lambda}_{MPB} &= \bar{\lambda}_{SPB} \int_0^{+\infty} \left\{ N(1-p(s))^{N(N-1)} + N(N-1)^2 p(s)(1-p(s))^{(N-1)^2} \right. \\ &\quad \left. + \sum_{k=1}^{N-2} \binom{N}{k} k \left[\sum_{h=1}^{N-k-1} \binom{N-k}{N-k-h} \binom{N-k}{N-k-h+1} (N-h-1) + k^2 \right] \right. \\ &\quad \left. \times p(s)^{N-k} (1-p(s))^{k(N-1)} \right\} f_{S_{SPB}}(s) ds \triangleq \bar{\lambda}_{SPB} \\ &\quad \times \int_0^{+\infty} \psi(N, p(s)) f_{S_{SPB}}(s) ds \end{aligned} \quad (4)$$

where $f_{S_{SPB}}(\cdot)$ denotes the probability density function⁵ of the sojourn time process of an arbitrary PU in Π . $p(s)$ denotes the conditioned probability of having at least one arrival A_i of $PU_i \in \Pi$ within the CR interference region during the sojourn time⁶ of $PU_j \in \Pi$, i.e., $p(s) \triangleq P(A_i \in S_j | S_j = s)$.

Proof. See Appendix A. \square

⁵ We assume that the sojourn time process is stationary, for this, there is no dependence in $f_s(\cdot)$ from the specific time slot.

⁶ Note that there is no dependence from the specific PUs involved in the evaluation of $f_{S_{SPB}}(\cdot)$ and $p(s)$ since the PU mobility patterns are assumed identically distributed.

Insight 1. Theorem 1 reveals that the average aggregate arrival rate $\bar{\lambda}_{\text{MPB}}$ is a non-linear function of N , as shown in Fig. 2. This is crucial since, as we prove in Section 5, the average aggregate arrival rate dominates the tuning of the sensing time parameters, and thus the CR spectrum opportunities. More specifically, the average aggregate arrival rate $\bar{\lambda}_{\text{MPB}}$ satisfies the following inequality:

$$\bar{\lambda}_{\text{MPB}} < N\bar{\lambda}_{\text{SPB}} \quad (5)$$

In fact, when $p(s) > 0$, we have $\int_0^{+\infty} \psi(N, p(s)) f_{S_{\text{SPB}}}(s) ds < N$. This result agrees with the reasonings in Remark 1.

We note that:

$$\lim_{p(s) \rightarrow 0} \bar{\lambda}_{\text{MPB}} = N\bar{\lambda}_{\text{SPB}} \quad (6)$$

This result is reasonable since, when $p(s) \rightarrow 0$, the PU arrivals do not belong to the sojourn times of the other PUs. Hence, the aggregated arrival rate is equal to the sum of the single arrival rates.

Corollary 1 (Average Aggregate Inter-Arrival Time). The average aggregate inter-arrival time \bar{T}_{MPB} of the PUs in Π roaming within the network region \mathbf{A} according to a general mobility model is given by:

$$\bar{T}_{\text{MPB}} = \frac{\bar{T}_{\text{SPB}}}{\int_0^{+\infty} \psi(N, p(s)) f_S(s) ds} \quad (7)$$

Proof. See Appendix B. \square

Remark 2. From (7), it results that \bar{T}_{MPB} depends on two factors: (i) the PU mobility model, through \bar{T}_{SPB} , $p(s)$ and $f_S(s)$; (ii) the number N of PUs that are sharing the same spectrum band. More in detail, \bar{T}_{MPB} depends through \bar{T}_{SPB} on the average PU velocity, the normalized protection radius R/a , and the size of the network region \mathbf{A} [6].

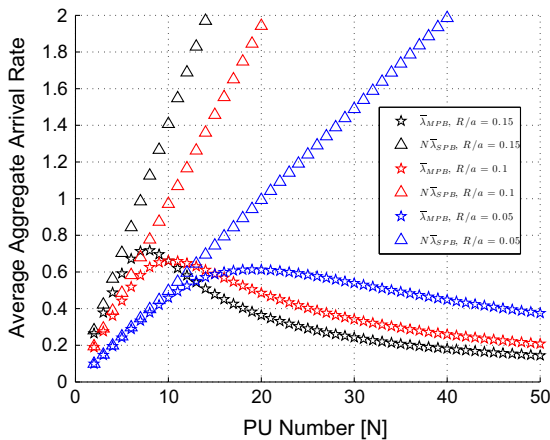


Fig. 2. Average aggregate arrival rate: non-linear dependence of $\bar{\lambda}_{\text{MPB}}$ on N . The curves are obtained by adopting the RWM model with normalized PU velocity v/a uniformly distributed in $[0.1, 0.9]$ for three different values of the normalized PU protection range R/a .

Remark 3. As stated before, $p(s)$ and $f_S(s)$ depend on the adopted PU mobility model. In particular, when the arrival counting process of the arbitrary PU_j is a Poisson process, the arrival time process has an Erlang distribution of parameter $\bar{\lambda}_{\text{SPB}}$. This assumption is verified by a very large number of mobility models, as for example the Random Walk Mobility (RWM) and its derivatives, the Random WayPoint Mobility (RWPM) and the Random Direction Mobility (RDM) models [6,12,19]. It is also verified by experimental mobility models based on human mobility as shown in [20–23]. In these cases, $p(s) = 1 - e^{-\bar{\lambda}_{\text{SPB}} s}$ and the sojourn time process has an exponential distribution with parameter $1/\bar{S}_{\text{SPB}}$.

Proposition 1 (Average Aggregate Sojourn Time). The average aggregate sojourn time \bar{S}_{MPB} of the PUs in Π roaming within the network region \mathbf{A} according to a general mobility model is given by:

$$\bar{S}_{\text{MPB}} = \frac{P(\mathcal{I}_{\text{MPB}}) \bar{T}_{\text{SPB}}}{\int_0^{+\infty} \psi(N, p(s)) f_S(s) ds} \quad (8)$$

Proof. See Appendix C. \square

Proposition 2 (Average Aggregate Out Time). The average aggregate out time $\bar{\Theta}_{\text{MPB}}$ of the PUs in Π roaming within the network region \mathbf{A} according to a general mobility model is given by:

$$\bar{\Theta}_{\text{MPB}} = \frac{P(\mathcal{O}_{\text{MPB}}) \bar{T}_{\text{SPB}}}{\int_0^{+\infty} \psi(N, p(s)) f_S(s) ds} \quad (9)$$

Proof. See Appendix D. \square

From Insight 1, the following two insights for the average aggregate sojourn time and for the average aggregate out time follow.

Insight 2. The average aggregate sojourn time \bar{S}_{MPB} satisfies the following inequality:

$$\bar{S}_{\text{MPB}} > \frac{P(\mathcal{I}_{\text{MPB}}) \bar{S}_{\text{SPB}}}{P(\mathcal{I}_{\text{SPB}}) N} \quad (10)$$

In fact, when $p(s) > 0$, $\bar{\lambda}_{\text{MPB}} < N\bar{\lambda}_{\text{SPB}}$. Hence, from (8), it follows $\bar{S}_{\text{MPB}} > \frac{P(\mathcal{I}_{\text{MPB}}) \bar{T}_{\text{SPB}}}{N}$. By accounting for $\bar{S}_{\text{SPB}} = \frac{P(\mathcal{I}_{\text{SPB}}) \bar{T}_{\text{SPB}}}{P(\mathcal{I}_{\text{SPB}})}$ [6], (10) follows. Clearly, when $p(s) \rightarrow 0$, by accounting for (6), one has $\bar{S}_{\text{MPB}} \rightarrow \frac{P(\mathcal{I}_{\text{MPB}}) \bar{S}_{\text{SPB}}}{P(\mathcal{I}_{\text{SPB}}) N}$.

Insight 3. The average aggregate out time $\bar{\Theta}_{\text{MPB}}$ satisfies the following inequality:

$$\bar{\Theta}_{\text{MPB}} > \frac{P(\mathcal{O}_{\text{MPB}}) \bar{\Theta}_{\text{SPB}}}{P(\mathcal{O}_{\text{SPB}}) N} \quad (11)$$

In fact, when $p(s) > 0$, $\bar{T}_{\text{MPB}} > \frac{\bar{T}_{\text{SPB}}}{N}$, from (8), it follows $\bar{\Theta}_{\text{MPB}} > \frac{P(\mathcal{O}_{\text{MPB}}) \bar{T}_{\text{SPB}}}{N}$. By accounting for $\bar{\Theta}_{\text{SPB}} = \frac{P(\mathcal{O}_{\text{SPB}}) \bar{T}_{\text{SPB}}}{P(\mathcal{O}_{\text{SPB}})}$

[6], (11) is obtained. Clearly, when $p(s) \rightarrow 0$, by accounting for (6), one has $\overline{\mathcal{O}}_{\text{MPB}} \rightarrow \frac{P(\mathcal{O}_{\text{MPB}})}{P(\mathcal{O}_{\text{SPB}})} \frac{\overline{\mathcal{O}}_{\text{SPB}}}{N}$.

Propositions 1 and 2 reveal that the evaluation of the average aggregate sojourn time $\overline{\mathcal{S}}_{\text{MPB}}$ and the average aggregate out time $\overline{\mathcal{O}}_{\text{MPB}}$ requires the knowledge of $P(\mathcal{I}_{\text{MPB}}) = 1 - P(\mathcal{O}_{\text{MPB}})$. In [11], $P(\mathcal{I}_{\text{MPB}})$ has been evaluated only for one-dimensional network regions and only for two mobility models. In the following, we derive a closed-form expression of $P(\mathcal{I}_{\text{MPB}})$ for bi-dimensional network regions and for a general mobility model. Then, we confer completeness to the analysis by providing more accurate closed-form expressions for two widely adopted mobility models, i.e., the RWPM and the RWM.

Proposition 3. *The probability $P(\mathcal{I}_{\text{MPB}})$ of a CR user being inside the protection range of at least one PU in Π , roaming within a two-dimensional network region $\mathbf{A} = [0, a] \times [0, a]$ according to a general mobility model, can be approximated when $R \ll a$ as follows:*

$$P(\mathcal{I}_{\text{MPB}}) = 1 - P(\mathcal{O}_{\text{MPB}}) \simeq 1 - \left(1 - \frac{\pi R^2}{a^2}\right)^N \quad (12)$$

Proof. See Appendix E. \square

Proposition 4. *The probability $P^{\text{RWM}}(\mathcal{I}_{\text{MPB}})$ of a CR user being inside the protection range of at least one PU in Π , roaming within a two-dimensional network region $\mathbf{A} = [0, a] \times [0, a]$ according to the RWM, can be approximated as follows:*

$$P^{\text{RWM}}(\mathcal{I}_{\text{MPB}}) = 1 - P^{\text{RWM}}(\mathcal{O}_{\text{MPB}}) \simeq 1 - \left(1 - \frac{\pi R^2}{a^2}\right)^N \quad (13)$$

Proof. See Appendix F. \square

(13) coincides with (12) due to the uniform steady-state spatial distribution of the PUs roaming according to the RWM model.

Proposition 5. *The probability $P^{\text{RWPM}}(\mathcal{I}_{\text{MPB}})$ of a CR user being inside the protection range of at least one PU in Π , roaming within a two-dimensional network region $\mathbf{A} = [0, a] \times [0, a]$ according to the RWPM, can be approximated as follows:*

$$\begin{aligned} P^{\text{RWPM}}(\mathcal{I}) &= 1 - P_{\text{MPB}}(\mathcal{O}) \\ &\simeq 1 - \frac{1}{a^2} \int \int_{\mathbf{A}} \left(1 - \frac{3\pi R^2}{2a^6} \left\{ [R^2 + 6y_{\text{CR}}(y_{\text{CR}} - a)] \right. \right. \\ &\quad \times \left. \left. [R^2 + 6x_{\text{CR}}(x_{\text{CR}} - a)] - 12x_{\text{CR}}y_{\text{CR}}(x_{\text{CR}} - a)(y_{\text{CR}} - a) \right\} \right)^N \\ &\quad \times dx_{\text{CR}} dy_{\text{CR}} \end{aligned} \quad (14)$$

Proof. See Appendix G. \square

5. Aggregate Primary-User: Criteria for tuning the sensing time parameters

Here, we derive the criteria for tuning the sensing time parameters when multiple PUs roaming in the network region are sharing the targeted spectrum band. Specifically, we provide closed-form expressions of the transmission time and the sensing time that jointly maximize the sensing efficiency and the sensing accuracy.

Proposition 6. *Let us consider the PUs in Π roaming within a network region \mathbf{A} according to a general mobility model. An arbitrary CR user, aiming to satisfy the PU interference constraint and to maximize the sensing efficiency for a given value of the sensing time, must set the transmission time $T_{\text{Tx}}^{\text{MPB}}$ as follows:*

$$T_{\text{Tx}}^{\text{MPB}} = \mathcal{F}_{T_{\text{MPB}}}^{-1} \left(\frac{\min_i \{P_{\text{int},i}\}}{1 - \prod_{i=1}^N P_{\text{off},i}} \right) \quad (15)$$

where $P_{\text{int},i}$ is the maximum interference probability tolerated by $\text{PU}_i \in \Pi$, $P_{\text{off},i}$ is the off-state probability of PU_i , and $\mathcal{F}_{T_{\text{MPB}}}(\cdot)$ is the cumulative distribution function of the aggregate inter-arrival time process.

Proof. See Appendix H. \square

Remark 4. As proved in Appendix H, the transmission time $T_{\text{Tx}}^{\text{MPB}}$ set according to Eq. (15) maximizes the sensing efficiency (Definition 5) for a given value of the sensing time, since $T_{\text{Tx}}^{\text{MPB}}$ is the maximum value of the transmission time satisfying the PU interference constraint.

Remark 5. From (15), it results that if the interference constraint $\min_i \{P_{\text{int},i}\}$ is equal to the probability that at least one of the N PUs in Π is active, i.e., $\min_i \{P_{\text{int},i}\} = P_{\text{on}}^{\text{MPB}} \triangleq 1 - \prod_{i=1}^N P_{\text{off},i}$, it results $T_{\text{Tx}}^{\text{MPB}} = \mathcal{F}_{T_{\text{MPB}}}^{-1}(1)$. This means that a CR user can transmit for an infinite time, as expected.

Corollary 2. *If the aggregate inter-arrival time process has an exponential distribution of parameter $\bar{\lambda}_{\text{MPB}}$, an arbitrary CR user, aiming to satisfy the PU interference constraint and to maximize the sensing efficiency for a given value of the sensing time, must set the transmission time $T_{\text{Tx}}^{\text{MPB}}$ as follows:*

$$\begin{aligned} T_{\text{Tx}}^{\text{MPB}} &= \bar{T}_{\text{MPB}} \log \left(\frac{1 - \prod_{i=1}^N P_{\text{off},i}}{1 - \prod_{i=1}^N P_{\text{off},i} - \min_i \{P_{\text{int},i}\}} \right) \\ &= \frac{\overline{\mathcal{O}}_{\text{MPB}}}{1 - P(\mathcal{I}_{\text{MPB}})} \\ &\quad \times \log \left(\frac{1 - \prod_{i=1}^N P_{\text{off},i}}{1 - \prod_{i=1}^N P_{\text{off},i} - \min_i \{P_{\text{int},i}\}} \right) \end{aligned} \quad (16)$$

Proof. See Appendix I. \square

Proposition 7. Let us consider the PUs in Π roaming within a network region \mathbf{A} according to a general mobility model. An arbitrary CR user, aiming to maximize the sensing accuracy, must set the sensing time T_s^{MPB} as follows:

$$T_s^{\text{MPB}} \leq \bar{\mathcal{S}}_{\text{MPB}} \quad (17)$$

where $\bar{\mathcal{S}}_{\text{MPB}}$ is the average aggregate sojourn time given in (8).

Proof. See Appendix J. \square

The rationale behind Proposition 7 is that observing the band for a time greater than the average aggregate sojourn time $\bar{\mathcal{S}}_{\text{MPB}}$ has two effects: (i) the probability P_d^{agg} of detecting the aggregate PU does not improve; (ii) the probability P_f^{agg} of false detecting the aggregate PU increases. Hence, in mobile scenarios, the sensing accuracy does not improve by observing the channel for sensing time longer than the average aggregate sojourn time $\bar{\mathcal{S}}_{\text{MPB}}$. This is an important result compared to static scenarios where it is well-known that longer sensing times lead to higher sensing accuracy.

Remark 6. We underline that the developed theoretical analysis implicitly accounts for the channel propagation conditions and the noise levels. In fact the decision variable Y and the threshold γ of the arbitrary adopted sensing technique determining the expressions of the detection P_d^{agg} and false-alarm P_f^{agg} probabilities (see Appendix J for details) depend on the adopted channel and noise models as shown in [24,25].

Remark 7. Result (17) holds regardless of the adopted spectrum sensing technique. Moreover, result (17) is reasonable. In fact, if an arbitrary CR user is out of the protection range of any PU in Π , i.e., if the event \mathcal{O}_{MPB} occurs, the CR user can use the band without interfering any PU in Π . So, it is useless to waste time by sensing a free band. Clearly, the amount of the average aggregate sojourn time to be devoted to the sensing depends on the specific sensing technique adopted. In particular, if $\bar{\mathcal{S}}_{\text{MPB}} \rightarrow 0$, $T_s^{\text{MPB}} \rightarrow 0$ as well. This agrees with the intuition: if the PUs are never in the CR interference region, it is useless to sense a free band.

6. Validation of the theoretical results

In this section, we first validate the derived analytical results by Monte Carlo simulations. Then, we show the effects of the different mobility parameters on the aggregate PU dynamics. This is crucial for the performance of a CR network, since as proved in Section 5, the aggregate PU mobility pattern dominates the tuning of the sensing time parameters.

We place uniformly 10^2 CR users in a bi-dimensional network region $\mathbf{A} = [0, a] \times [0, a]$. The PUs move according to the RWM model and the RDM model for enough time to assure 10^3 inter-arrival events. Moreover, they start their movements from the steady-state spatial distribution

and they randomly choose the normalized velocity v/a according to a uniform distribution in the interval $[0.1, 0.9]$ m/s. Finally, the normalized protection range R/a of the arbitrary PU in Π is set equal to two different values in order to confer generality to the analysis, i.e., 0.01 and 0.02.

Fig. 3 shows the average aggregate inter-arrival time \bar{T}_{MPB} vs the number N of PUs in Π , for both the considered mobility models. The analytical results evaluated according to (7) match well the simulation results, for both the considered mobility models. In particular, we note that \bar{T}_{MPB} is a non-linear function of the number N of PUs, in agreement with Insight 1.

Figs. 4 and 5 show the sensing time T_s^{MPB} and the transmission time $T_{\text{Tx}}^{\text{MPB}}$ as the number of PUs in Π increases, for both the considered mobility models. We set $\min_i \{P_{\text{int},i}\} = 10^{-2}$ and $P_{\text{off},i} = 2/3 \forall i = 1, \dots, N$. The analytical results are obtained by setting T_s^{MPB} according to the upper bound derived in Proposition 7, i.e., $T_s^{\text{MPB}} = \bar{\mathcal{S}}_{\text{MPB}}$.

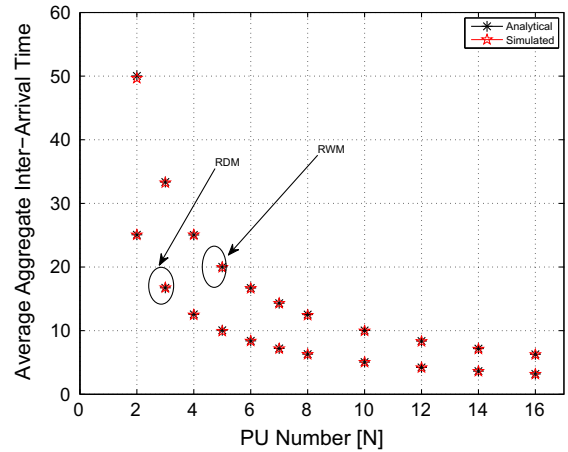


Fig. 3. Average aggregate inter-arrival time vs the number N of PUs.

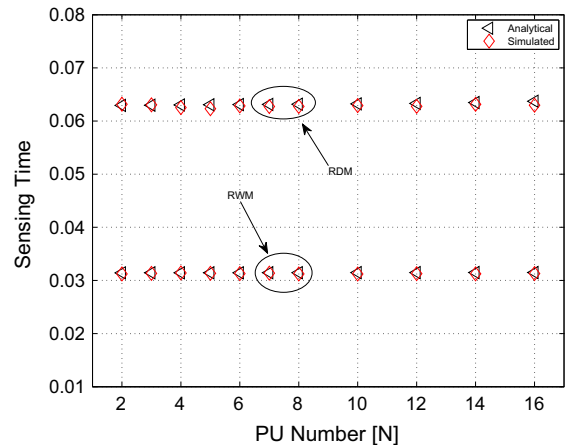


Fig. 4. Sensing time vs the number N of PUs.

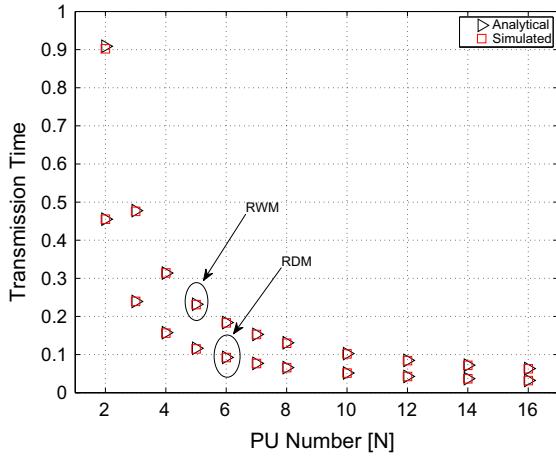


Fig. 5. Transmission time vs the number N of PUs.

and by setting T_{Tx}^{MPB} according to (16). We note that the theoretical results match well the simulation results, for both the considered mobility models. In particular, with reference to the sensing time, T_s^{MPB} is a non-linear function of the number N of PUs. Furthermore, we observe that the curve trend appears almost constant, since the normalized protection range $R/a \ll 1$, i.e., $R/a = 0.01$ and $R/a = 0.02$, and hence $P(\mathcal{I}_{MPB})$ derived in (12) is very small. Finally, with reference to the transmission time, when N increases, T_{Tx}^{MPB} decreases non-linearly. This behavior is due to two factors: (i) the decreasing of the aggregate inter-arrival time as N increases; (ii) the increasing of the probability of the aggregate PU being active as N increases.

Figs. 6 and 7 depict the instantaneous interference levels produced by a CR user on the aggregate PU transmissions for the RWM and the RDM mobility models, respectively. The horizontal red line represents $\min_i \{P_{int,i}\} = 10^{-2}$. The results confirm the benefits of setting the transmission time according to the theoretical result, for both the considered mobility models. In particular, the average interference levels (obtained by averaging

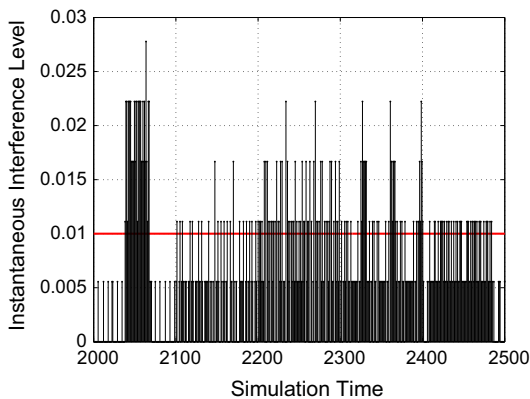


Fig. 6. Aggregate instantaneous interference level for the RWM as function of time.

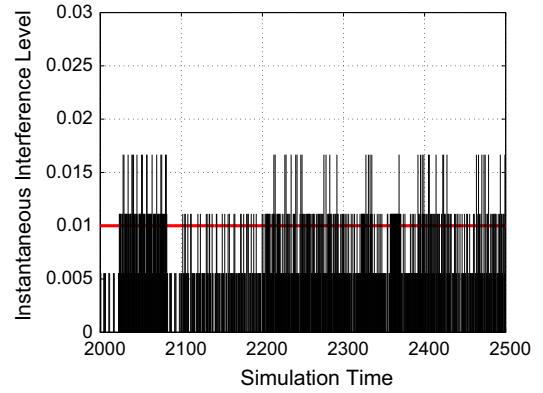


Fig. 7. Aggregate instantaneous interference level for the RDM as function of time.

the instantaneous interference levels over the simulation time) on the aggregate PU transmissions are equal to $0.00998 \approx 10^{-2}$ for the RWM and $0.0099 \approx 10^{-2}$ for the RDM, in agreement with Proposition 6.

Now, we show the effects of the different mobility parameters on the aggregate PU dynamics, since this is crucial for the tuning of the sensing time parameters. To this aim, let us consider Figs. 8–10 that report the average aggregate inter-arrival time \bar{T}_{MPB} , the average aggregate sojourn time \bar{S}_{MPB} and the average aggregate out time \bar{O}_{MPB} vs the number of PUs in Π , for three different values of the normalized protection range, i.e., $R/a = 0.15$, $R/a = 0.1$ and $R/a = 0.05$, when the RWM is adopted.

First, we note that the aggregate inter-arrival time has a concave behavior as function of N . This is due to the opposite behaviors of the aggregate sojourn time and the aggregate out time as function of N . Specifically, when N increases, \bar{S}_{MPB} increases, whereas \bar{O}_{MPB} decreases. However, the two curves exhibit different slopes. This means that, for small values of N , the decreasing of the aggregate out time dominates the increasing of the

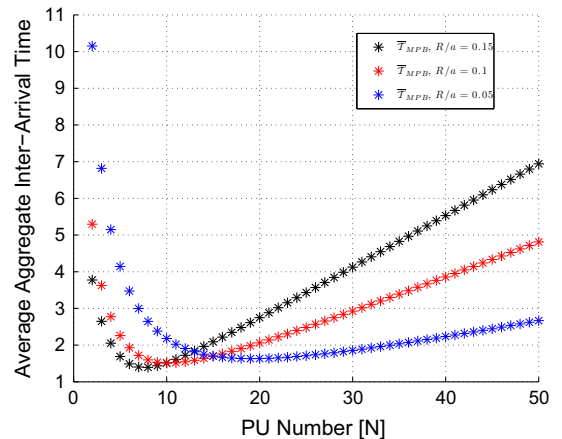


Fig. 8. Average aggregate inter arrival time.

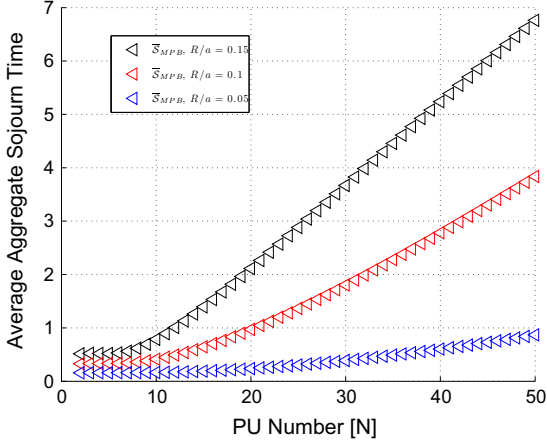


Fig. 9. Average aggregate sojourn time.

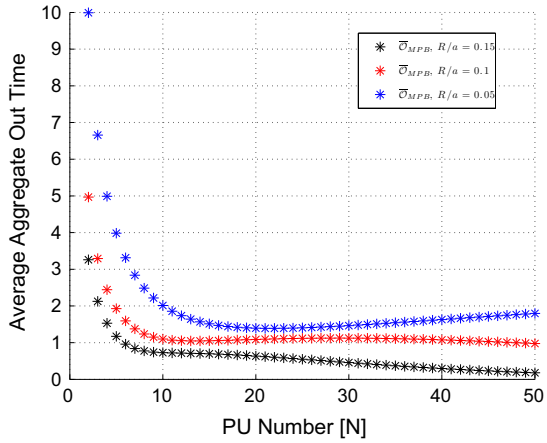


Fig. 10. Average aggregate out time.

aggregate sojourn time. As a consequence, the aggregate inter-arrival time decreases. Differently, for higher values of N , the increasing of the aggregate sojourn time dominates the decreasing of the aggregate out time. As a consequence, the aggregate inter-arrival time increases. The value of N for which the aggregate inter-arrival time inverts its behavior depends on the PUs mobility parameters, as shown in Fig. 8. Specifically, as the normalized protection range R/a increases, such a value of N decreases. The reason is that, when R/a increases, the probability of a CR user being inside the aggregate PU protection range increases as well. Similarly, as the average PU velocity decreases, the value of N for which the aggregate inter-arrival time inverts its behavior decreases as well, since the time the aggregate PU spends inside the CR interference region increases.

7. Conclusions

The emerging applications of the small-scale primary-user (PU) paradigm requires Cognitive Radio (CR) networks to explicitly support the mobility of a

multitude of PUs concurrently using the same spectrum band. Hence, in this paper, we answered the following fundamental questions to jointly maximize the sensing efficiency and the sensing accuracy in presence of multiple mobile PUs: (i) How long can a CR user transmit without interfering with the multiple mobile PUs? (ii) How long must a CR user observe a targeted spectrum band to reliably detect multiple mobile PUs? For this, we first proposed the aggregate PU model to effectively describe the cumulative effects of multiple mobile PUs on the spectrum sensing functionality. Then, stemming from this model, we derive closed-form expressions for the *sensing time* and the *transmission time* that jointly maximize the sensing efficiency and the sensing accuracy. We derived all the theoretical results by adopting a general mobility model for the multiple PUs, and we validated the analytical results through simulations.

Appendix A. Proof of Theorem 1

Let us consider the case $N = 3$. By accounting for the aggregate PU model developed in Section 4, a realization of the aggregate arrival rate is given by⁷:

$$\lambda_{MPB} = \left\{ \begin{array}{l} \underbrace{\lambda_i}_{i \in (1,2,3)}, \quad \text{if } \left\{ \bigcap_{\substack{j=1 \\ j \neq i}}^3 \{A_j \in S_i = s_i, A_i \notin S_j = s_j\} \cup \right. \\ \left. \bigcup_{\substack{j=1 \\ j \neq i}}^3 \left\{ A_j \in S_i = s_i, A_i \notin S_j = s_j, \bigcap_{\substack{k=1 \\ k \neq j}}^3 \{A_k \in S_j = s_j, \right. \right. \right. \\ \left. \left. \left. A_k \notin S_i = s_i\} \right\} \right\} \\ \underbrace{\lambda_i + \lambda_j}_{(i,j) \in (1,2,3), i \neq j}, \quad \text{if } \left\{ A_i \notin S_j = s_j, A_j \notin S_i = s_i, \bigcap_{\substack{k=1 \\ k \neq i}}^3 \{A_i \notin S_k = s_k, \right. \\ \left. A_j \notin S_k = s_k, \left\{ \bigcup_{l=1}^3 A_l \in S_l = s_l \right\} \right\} \\ \lambda_1 + \lambda_2 + \lambda_3, \quad \text{if } \left\{ \bigcap_{i=1}^3 \left\{ \bigcap_{\substack{j=1 \\ j \neq i}}^3 A_i \notin S_j = s_j \right\} \right\} \end{array} \right\} \quad (\text{A.1})$$

By accounting for the equal distribution and for the independence of the PU mobility patterns, the conditioned average value of λ_{MPB} is given by:

⁷ In (A.1), we have denoted with $\{B \cap C\}$ or equivalently with $\{B, C\}$ the intersection between the events B and C . Moreover, we have denoted with $\{B \cup C\}$ the union of the events B and C .

$$\begin{aligned} \psi(N, p(s)) &\triangleq E[\lambda_{\text{MPB}} | S=s] = 3\bar{\lambda}_{\text{SPB}}(1-p(s))^6 + 12\bar{\lambda}_{\text{SPB}}p(s)(1-p(s))^4 + 9\bar{\lambda}_{\text{SPB}}p(s)^2(1-p(s))^2 \\ &= \bar{\lambda}_{\text{SPB}} \left\{ N(1-p(s))^{N(N-1)} + Np(s)(1-p(s))^{N-1} (N-1)^2 + \binom{N}{1} \overbrace{\left[\sum_{h=1}^{N-1} \binom{N-1}{N-1-h} \binom{N-1}{N-1-h+1} (N-h-1) + 1 \right]}^3 p(s)^{N-1} (1-p(s))^{1(N-1)} \right\} \end{aligned} \quad (\text{A.2})$$

The average value of λ_{MPB} is finally obtained as $\bar{\lambda}_{\text{MPB}} = \int_0^{+\infty} E[\lambda_{\text{MPB}} | S=s] f_{S_{\text{SPB}}}(s) ds \triangleq \int_0^{+\infty} \psi(N, p(s)) f_{S_{\text{SPB}}}(s) ds$. Thus, for an arbitrary value of N , the proof easily follows by adopting similar reasonings and by enumerating all the possible events as in (A.1).

Appendix B. Proof of Corollary 1

Since $\bar{\mathcal{T}}_{\text{MPB}} = \frac{1}{\bar{\lambda}_{\text{MPB}}}$, stemming from (4) and by accounting for $\bar{\mathcal{T}}_{\text{SPB}} = \frac{1}{\bar{\lambda}_{\text{SPB}}}$, the proof follows.

Appendix C. Proof of Proposition 1

By accounting for the aggregate PU model developed in Section 4, the overall inter-arrival time process of the N PUs in Π roaming in a network region \mathbf{A} is equivalent to the inter-arrival time process of a single aggregate PU roaming in the same network region. Thus, by using Little's Theorem [18], the average aggregate sojourn time \bar{S}_{MPB} is given by:

$$\bar{S}_{\text{MPB}} = P(\mathcal{I}_{\text{MPB}}) \bar{\mathcal{T}}_{\text{MPB}} \quad (\text{C.1})$$

where $P(\mathcal{I}_{\text{MPB}})$ is derived in (3). By substituting (7) in (C.1), the proof follows.

Appendix D. Proof of Proposition 2

By accounting for Definition 7 and (8), one has:

$$\begin{aligned} \bar{\mathcal{O}}_{\text{MPB}} &= \bar{\mathcal{T}}_{\text{MPB}} - \bar{S}_{\text{MPB}} = (1 - P_{\text{MPB}}(\mathcal{I})) \bar{\mathcal{T}}_{\text{MPB}} \\ &= P(\mathcal{O}_{\text{MPB}}) \bar{\mathcal{T}}_{\text{MPB}} \end{aligned} \quad (\text{D.1})$$

By substituting (7) in (D.1), the proof follows.

Appendix E. Proof of Proposition 3

If $R \ll a$, $P(\mathcal{I}_{\text{SPB}} | \mathbf{x}_{\text{CR}})$ can be assumed independent of \mathbf{x}_{CR} . As a consequence, from (3), one has:

$$P(\mathcal{I}_{\text{MPB}}) \simeq 1 - (1 - P(\mathcal{I}_{\text{SPB}} | \mathbf{x}_{\text{CR}}))^N \quad (\text{E.1})$$

where $P(\mathcal{I}_{\text{SPB}} | \mathbf{x}_{\text{CR}})$ can be easily evaluated as the fraction of the network region covered by the arbitrary PU, i.e., $P(\mathcal{I}_{\text{SPB}} | \mathbf{x}_{\text{CR}}) \simeq \frac{\pi R^2}{a^2}$.

Appendix F. Proof of Proposition 4

By neglecting the border effects, i.e., by supposing $R \ll a$, $P(\mathcal{I}_{\text{SPB}} | \mathbf{x}_{\text{CR}})$ in (3) can be calculated as follows:

$$\begin{aligned} P(\mathcal{I}_{\text{SPB}} | \mathbf{x}_{\text{CR}}) &\triangleq \int \int_{\mathcal{C}(\mathbf{x}_{\text{CR}})} f_{\mathbf{x}_{\text{PU}}}(\mathbf{x}_{\text{PU}}) d\mathbf{x}_{\text{PU}} \\ &\simeq \int_{y_{\text{CR}}-R}^{y_{\text{CR}}+R} \int_{x_{\text{CR}}-\sqrt{R^2-(t-y_{\text{CR}})^2}}^{x_{\text{CR}}+\sqrt{R^2-(t-y_{\text{CR}})^2}} f_{\mathbf{x}_{\text{PU}}}(z, t) dz dt \end{aligned} \quad (\text{F.1})$$

By substituting in (F.1) the expressions of the PU spatial distributions for the RWM in the two-dimensional case [26] and by using the notable relations [27] $\int \sin^m(\alpha) d\alpha = -\frac{\cos(\alpha) \sin^{m-1}(\alpha)}{m} + \frac{m-1}{m} \int \sin^{m-2}(\alpha) d\alpha$ and $\int \cos^m(\alpha) d\alpha = \frac{\sin(\alpha) \cos^{m-1}(\alpha)}{m} + \frac{m-1}{m} \int \cos^{m-2}(\alpha) d\alpha$, one obtains:

$$P^{\text{RWM}}(\mathcal{I}_{\text{SPB}} | \mathbf{x}_{\text{CR}}) \simeq \frac{\pi R^2}{a^2} \quad (\text{F.2})$$

By substituting (F.2) in (3), the proof follows.

Appendix G. Proof of Proposition 5

By neglecting the border effects, i.e., by supposing $R \ll a$, $P(\mathcal{I}_{\text{SPB}} | \mathbf{x}_{\text{CR}})$ in (3) can be written as in (F.1). By substituting in (F.1) the expressions of the PU spatial distributions for the RWPM in the two-dimensional case [28] and by using the notable relations [27] $\int \sin^m(\alpha) d\alpha = -\frac{\cos(\alpha) \sin^{m-1}(\alpha)}{m} + \frac{m-1}{m} \int \sin^{m-2}(\alpha) d\alpha$ and $\int \cos^m(\alpha) d\alpha = \frac{\sin(\alpha) \cos^{m-1}(\alpha)}{m} + \frac{m-1}{m} \int \cos^{m-2}(\alpha) d\alpha$, one obtains:

$$\begin{aligned} P^{\text{RWPM}}(\mathcal{I}_{\text{SPB}} | \mathbf{x}_{\text{CR}}) &\simeq \frac{3\pi R^2}{2a^6} \left\{ [R^2 + 6y_{\text{CR}}(y_{\text{CR}} - a)] \right. \\ &\quad \times [R^2 + 6x_{\text{CR}}(x_{\text{CR}} - a)] \\ &\quad \left. - 12x_{\text{CR}}y_{\text{CR}}(x_{\text{CR}} - a)(y_{\text{CR}} - a) \right\} \end{aligned} \quad (\text{G.1})$$

By substituting (G.1) in (3) and by accounting for the uniform distribution of the CR users, the proof follows.

Appendix H. Proof of Proposition 6

By accounting for the aggregate PU model developed in Section 4, we can adopt similar reasonings as in [6] for setting the transmission time allowing a CR user to respect the PU interference constraint and maximizing the sensing efficiency for a given value of the sensing time. Specifically, during two aggregate PU arrival events in a CR interference

region, a CR user can interfere the active aggregate PU during the transmission time. As a consequence, the CR transmission time cannot exceed the maximum interference time the active aggregate PU can tolerate between two arrival events, i.e., it cannot exceed the minimum of the maximum interference times the active PUs in Π can individually tolerate. Moreover, the aggregate PU is active when at least one of the N PUs in Π is active. This event has probability $P_{\text{on}}^{\text{MPB}} \triangleq 1 - \prod_{i=1}^N P_{\text{off},i}$. As a consequence, we have:

$$\begin{aligned} \mathcal{F}_{T_{\text{MPB}}}(T_{\text{Tx}})P_{\text{on}}^{\text{MPB}} &= P(T_{\text{MPB}} \leq T_{\text{Tx}})P_{\text{on}}^{\text{MPB}} \leq \min_i \{P_{\text{int},i}\} \\ \Leftrightarrow T_{\text{Tx}} &\leq \mathcal{F}_{T_{\text{MPB}}}^{-1} \left(\frac{\min_i \{P_{\text{int},i}\}}{P_{\text{on}}^{\text{MPB}}} \right) \end{aligned} \quad (\text{H.1})$$

and the proof follows by considering the maximum T_{Tx} satisfying (H.1).

Appendix I. Proof of Corollary 2

If the aggregate inter-arrival process has an exponential distribution of parameter $\bar{\lambda}_{\text{MPB}}$, then $\mathcal{F}_{T_{\text{MPB}}}(t) = 1 - e^{-\bar{\lambda}_{\text{MPB}} t}$. Hence, the proof follows by accounting for (9) and (15).

Appendix J. Proof of Proposition 7

By accounting for the aggregate PU model developed in Section 4, we can adopt similar reasonings as in [6] for setting the sensing time. Specifically, Y and γ denote the decision variable and the threshold of a generic sensing technique, respectively. $\mathcal{H}_0^{\text{agg}}$ and $\mathcal{H}_1^{\text{agg}}$ denote the hypotheses of “no aggregate PU signal” and “aggregate PU signal transmitted”, respectively. The detection probability $P_d^{\text{agg}} \triangleq P(Y > \gamma | \mathcal{H}_1^{\text{agg}})$ is affected only by the event \mathcal{I}_{MPB} , since if the event \mathcal{O}_{MPB} occurs, the CR user cannot sense any PU in Π . Instead, the false-alarm probability $P_f^{\text{agg}} \triangleq P(Y > \gamma | \mathcal{H}_0^{\text{agg}})$ is affected by both the events \mathcal{I}_{MPB} and \mathcal{O}_{MPB} . Specifically:

$$P_d^{\text{agg}} = P(Y > \gamma | \mathcal{H}_1^{\text{agg}}, \mathcal{I}_{\text{MPB}})P(\mathcal{I}_{\text{MPB}}) \quad (\text{J.1})$$

$$\begin{aligned} P_f^{\text{agg}} &= P(Y > \gamma | \mathcal{H}_0^{\text{agg}}, \mathcal{I}_{\text{MPB}})P(\mathcal{I}_{\text{MPB}}) \\ &\quad + P(Y > \gamma | \mathcal{H}_0^{\text{agg}}, \mathcal{O}_{\text{MPB}})P(\mathcal{O}_{\text{MPB}}) \\ &\geq P(Y > \gamma | \mathcal{H}_0^{\text{agg}}, \mathcal{I}_{\text{MPB}})P(\mathcal{I}_{\text{MPB}}) \end{aligned} \quad (\text{J.2})$$

with $P(\mathcal{I}_{\text{MPB}}) = \bar{\delta}_{\text{MPB}}/\bar{T}_{\text{MPB}}$. From (J.1) and (J.2), it results that observing the band for a time greater than the average aggregate sojourn time $\bar{\delta}_{\text{MPB}}$ has two effects: (i) P_d^{agg} does not improve; (ii) P_f^{agg} can increase. Hence, for an efficient spectrum sensing, T_s^{MPB} has to be set by accounting only for $\bar{\delta}_{\text{MPB}}$.

References

- [1] I.F. Akyildiz, B.F. Lo, R. Balakrishnan, Cooperative spectrum sensing in cognitive radio networks: a survey, *Phys. Commun. (Elsevier)* J. 4 (2011) 40–62.
- [2] I.F. Akyildiz, W.Y. Lee, K.R. Chowdhury, CRAHNs: cognitive radio ad hoc networks, *Ad Hoc Netw. (Elsevier)* J. 7 (5) (2009) 810–836.
- [3] W.Y. Lee, I. Akyildiz, Optimal spectrum sensing framework for cognitive radio networks, *IEEE Trans. Wireless Commun.* 7 (10) (2008) 3845–3857.
- [4] A. Ghasemi, E.S. Sousa, Optimization of spectrum sensing for opportunistic spectrum access in cognitive radio networks, in: *IEEE Consumer Commun. and Networking Conference (CCNC)*, 2007, pp. 1022–1026.
- [5] Y.C. Liang, Y. Zeng, E.C. Peh, A.T. Hoang, Sensing-throughput tradeoff for cognitive radio networks, *IEEE Trans. Wireless Commun.* 7 (4) (2008) 1326–1337.
- [6] A.S. Cacciapuoti, I.F. Akyildiz, L. Paura, Optimal primary-user mobility aware spectrum sensing design for cognitive radio networks, *IEEE J. Sel. Areas Commun. (JSAC)* 31 (11) (2013) 2161–2172.
- [7] E. Peh, Y.C. Liang, Y.L. Guan, Y. Zeng, Power control in cognitive radios under cooperative and non-cooperative spectrum sensing, *IEEE Trans. Wireless Commun.* 10 (12) (2011) 4238–4248.
- [8] A.S. Cacciapuoti, M. Caleffi, L. Paura, R. Savoia, Decision maker approaches for cooperative spectrum sensing: participate or not participate in sensing?, *IEEE Trans Wireless Commun.* 12 (5) (2013) 2445–2457.
- [9] K.W. Choi, E. Hossain, D.I. Kim, Cooperative spectrum sensing under a random geometric primary user network model, *IEEE Trans. Wireless Commun.* 10 (6) (2011) 1932–1944.
- [10] A.S. Cacciapuoti, I.F. Akyildiz, L. Paura, Correlation-aware user selection for cooperative spectrum sensing in cognitive radio ad hoc networks, *IEEE J. Sel. Areas Commun. (JSAC)* 30 (2) (2012) 297–306.
- [11] A.S. Cacciapuoti, I.F. Akyildiz, L. Paura, Primary-user mobility impact on spectrum sensing in cognitive radio networks, in: *Proc. of IEEE Symposium on Personal, Indoor, Mobile and Radio Communications (PIMRC)*, 2011, pp. 451–456.
- [12] T. Camp, J. Boleng, V. Davies, A survey of mobility models for ad hoc network research, *Wireless Commun. Mob. Comput.* 2 (5) (2002) 483–502.
- [13] M. Caleffi, I.F. Akyildiz, L. Paura, OPERA: optimal routing metric for cognitive radio ad hoc networks, *IEEE Trans. Wireless Commun.* 11 (8) (2012) 2884–2894.
- [14] K. Xu, M. Gerla, S. Bae, How effective is the IEEE 802.11 RTS/CTS handshake in ad hoc networks, in: *Proc. of IEEE Global Telecommunications Conference (GLOBECOM)*, 2002.
- [15] H. Cai, D.Y. Eun, Crossing over the bounded domain: from exponential to power-law intermeeting time in mobile ad hoc networks, *IEEE/ACM Trans. Netw.* 17 (5) (2009).
- [16] C. Bettstetter, On the connectivity of ad hoc networks, *Comput. J.* 47 (4) (2004) 432–447.
- [17] A.S. Cacciapuoti, M. Caleffi, Interference analysis for secondary coexistence in TV white space, *IEEE Commun. Lett.* 19 (3) (2015) 383–386, <http://dx.doi.org/10.1109/LCOMM.2014.2386349>.
- [18] S.M. Ross, *Introduction to Probability Models*, Academic Press, 2000.
- [19] M. Caleffi, L. Paura, M-DART: multi-path dynamic address routing, *Wireless Commun. Mob. Comput.* 11 (3) (2011) 392–409, <http://dx.doi.org/10.1002/wcm.986>.
- [20] P. Hui, A. Chaintreau, J. Scott, R. Gass, J. Crowcroft, C. Diot, Pocket switched networks and human mobility in conference environments, in: *Proc. of ACM SIGCOMM Workshop on Delay-Tolerant Networking (WDTN)*, 2005.
- [21] J. Leguay, A. Lindgren, J. Scott, T. Friedman, J. Crowcroft, Opportunistic content distribution in an urban setting, in: *Proc. of ACM SIGCOMM workshop on Challenged networks (CHANTS)*, 2006.
- [22] A.S. Cacciapuoti, F. Calabrese, M. Caleffi, G.D. Lorenzo, L. Paura, Human-mobility enabled networks in urban environments: is there any (mobile wireless) small world out there?, *Ad Hoc Netw. (Elsevier)* J. 10 (8) (2012) 1520–1531.
- [23] A.S. Cacciapuoti, F. Calabrese, M. Caleffi, G.D. Lorenzo, L. Paura, Human-mobility enabled wireless networks for emergency communications during special events, *Pervasive Mob. Comput. (Elsevier)* J. 9 (4) (2013) 472–483.
- [24] A. Mariani, A. Giorgetti, M. Chiani, Effects of noise power estimation on energy detection for cognitive radio applications, *IEEE Trans. Commun.* 59 (12) (2011) 3410–3420.
- [25] A. Mariani, S. Kandeepan, A. Giorgetti, Periodic spectrum sensing with non-continuous primary user transmissions, *IEEE Trans. Wireless Commun.* 14 (3) (2015) 1636–1649.
- [26] J.Y.L. Boudec, M. Vojnovic, Perfect simulation and stationarity of a class of mobility models, in: *Proc. of IEEE INFOCOM*, vol. 4, 2005.
- [27] M. Abramowitz, I. Stegun, *Handbook of Mathematical Functions with Formulas, Graphs, and Mathematical Tables*, Dover Publications, New York, 1972.

- [28] C. Bettstetter, H. Hartenstein, X. Perez-Costa, Stochastic properties of the random waypoint mobility model, *Wireless Netw.* 10 (2004) 555–567.



Angela Sara Cacciapuoti received the Dr. Eng. degree *summa cum laude* in Telecommunications Engineering in 2005, and the Ph.D degree with score “excellent” in Electronic and Telecommunications Engineering in 2009, both from University of Naples Federico II. Currently, she is an Assistant Professor with the Department of Electrical Engineering and Information Technologies (DIETI), University of Naples Federico II. Dr. Cacciapuoti is an Area Editor of *Computer Networks (ELSEVIER) Journal*. From

2010 to 2011, she has been with the Broadband Wireless Networking Laboratory, Georgia Institute of Technology, as visiting researcher. In 2011, Dr. Cacciapuoti has also been with the NaNoNetworking Center in Catalunya (N3Cat), Universitat Politècnica de Catalunya (UPC), as visiting

researcher. Her current research interests are in cognitive radio networks and nanonetworks.



Marcello Caleffi received the Dr. Eng. degree (*summa cum laude*) in computer science engineering from the University of Lecce, Lecce, Italy, in 2005, and the Ph.D. degree in electronic and telecommunications engineering from the University of Naples Federico II, Naples, Italy, in 2009. Currently, he is an Assistant Professor with the Department of Electrical Engineering and Information Technologies, University of Naples Federico II. From 2010 to 2011, he was with the Broadband Wireless Networking Laboratory,

Georgia Institute of Technology, Atlanta, GA, USA, as a Visiting Researcher. In 2011, he was also with the NaNoNetworking Center in Catalunya (N3Cat), Universitat Politècnica de Catalunya (UPC), Barcelona, Spain, as a Visiting Researcher. He serves as area editor for *Elsevier Ad Hoc Networks*. His research interests are in cognitive radio networks and biological networks.